

Dichotomy between Level Broadening and Level Coupling to Electrodes in Large Area EGaIn Molecular Junctions

Ioan Bâldea*

Theoretical Chemistry, Heidelberg University, Im Neuenheimer Feld 229, D-69120 Heidelberg, Germany

E-mail: ioan.baldea@pci.uni-heidelberg.de

Abstract

Choosing self-assembled monolayers (SAM) of fluorine terminated oligophenylenes adsorbed on gold as illustration, we show that a single level (molecular orbital, MO) model can excellently reproduce full I - V curves measured for large area junctions fabricated with top EGaIn contact. In addition, this model unravels a surprising dichotomy between MO coupling to electrodes and the MO broadening. Importantly for the coherence of the microscopic description, the latter is found to correlate with the SAM coverage and molecular and π^* orbital tilt angles.

Interrogating the role of the platform of fabricating molecular junctions on the transport properties represents an important issue for molecular electronics. One may ask, for example, whether large area molecular junctions can also be quantitatively described within the dominant transport channel scenario,¹⁻²⁹ which succeeded to provide a coherent microscopical description of single-molecule junctions obtained via mechanically controlled (MC-BJ)³⁰ and scanning tunneling microscope (STM-BJ) break junctions⁵ or conducting probe atomic force microscopy (CP-AFM),^{22-24,31}

To analyze transport data for large area molecular junctions, which is the present aim of this Letter, we will combine results deduced recently^{32,33} expressing the tunneling current density J mediated by a single (dominant) molecular orbital (MO) at different levels of theory yielding the following formulas

$$J_{exact} = \frac{2\pi k_B T \sigma}{e \operatorname{Re} \psi' \left(\frac{1}{2} + i \frac{\varepsilon_0}{2\pi k_B T} \right)} \left[\operatorname{Im} \psi \left(\frac{1}{2} + \frac{\Lambda}{2\pi k_B T} + i \frac{\varepsilon_V + eV/2}{2\pi k_B T} \right) - \operatorname{Im} \psi \left(\frac{1}{2} + \frac{\Lambda}{2\pi k_B T} + i \frac{\varepsilon_V - eV/2}{2\pi k_B T} \right) \right] \quad (1a)$$

$$J_{0K} = \sigma \frac{\varepsilon_0^2 + \Lambda^2}{e\Lambda} \left(\arctan \frac{\varepsilon_V + eV/2}{\Lambda} - \arctan \frac{\varepsilon_V - eV/2}{\Lambda} \right) \quad (1b)$$

$$J_{0K, \text{off}} = \sigma \frac{\varepsilon_0^2}{\varepsilon_V^2 - (eV/2)^2} V \quad (1c)$$

$$\varepsilon_V = \varepsilon_0 + \gamma eV$$

Above, ψ and ψ' are Euler's digamma and trigamma functions of complex argument,³⁴ ε_0 represents the MO energy offset (which is negative in the specific case of the phenylene-based molecular junctions where conduction proceeds via the HOMO,³¹ $\varepsilon_0 = -|\varepsilon_0|$), γ is the strength of the MO bias driven shift, Λ is the (HO)MO width (see below), and T ($= 298.12$ K) and k_B are the (room) temperature and Boltzmann's constant, respectively.

The expressions of the low bias conductivity σ utilized at arriving at eq (1a), (1b), and (1c) read, respectively³²

$$\sigma_{exact} = G_0 \frac{\bar{\Gamma}^2}{2\pi\Lambda k_B T} \operatorname{Re} \psi' \left(\frac{1}{2} + \frac{\Lambda + i\varepsilon_0}{2\pi k_B T} \right) \quad (2a)$$

$$\sigma_{0K} = G_0 \frac{\bar{\Gamma}^2}{\varepsilon_0^2 + \Lambda^2} \quad (2b)$$

$$\sigma_{0K, \text{off}} = G_0 \frac{\bar{\Gamma}^2}{\varepsilon_0^2} \quad (2c)$$

The quantity

$$\bar{\Gamma}^2 = \frac{N_{\text{eff}}}{\mathcal{A}} \Gamma^2 \quad (3)$$

is related to the (geometric) average MO coupling $\Gamma = \sqrt{\Gamma_s \Gamma_t}$ to the two (substrate s and top t) electrodes by a factor accounting for the fact that in large area molecular junctions with eutectic gallium indium alloy (EGaIn) top electrodes only a tiny amount of the total number of molecules N_{eff} per geometric area \mathcal{A} are current carrying.^{35,36}

As emphasized recently^{32,33} and exemplary confirmed below, along with the MO couplings to the two (substrate s and top t) electrodes $\Gamma_{s,t}$, the MO width Λ can and does also contain a significant “extrinsic” contribution Γ_{env} not related with molecule-electrode interactions

$$\Lambda = \frac{1}{2} (\Gamma_s + \Gamma_t + \Gamma_{\text{env}}) \quad (4)$$

Within the assumption of a single dominant level, eq (1a) is exact for arbitrary biases and temperatures.³³ Eqs (1b) represents an accurate approximation of eq (1a) at sufficiently low temperatures. Eqs (1c) accurately reproduces eq (1b) at biases sufficiently far away from resonant tunneling.

Most applications of the single level model to date comprise molecular junctions anchored with thiols or possessing a hydrogen atom at the physical contact.^{5,23,24,31} To emphasize the generality of the description based on the single level model, we will consider as a specific application large area EGaIn-based molecular tunnel junctions fabricated with the oligophenylene thiol homologous series ($n = 1, 2, 3$) wherein the terminal hydrogen atom is substituted by a fluorine atom (F-nPT).³⁷

The fact that, out of the various tail group (H→R=F, CH₃, CF₃) substitutions investigated experimentally,³⁷ fluorination (R=F) yielded the most pronounced changes in the transport properties as compared to the nonsubstituted oligophenyl thiols (H-nPT) is one reason for this choice. Another reason is the intrinsic electronegativity of the F atom, which could act as a charge trap at the physisorbed contact,^{37,38} possibly giving rise to additional Coulomb interactions at contacts escaping the framework based on the single level model (referred to as the “(non)interacting” single

level model in the many-body community^{39–42}).

The parameter values adjusted by fitting the experimental J – V data for F-nPT junctions³⁷ to eq (1a), (1b), and (1c) are collected in Table 1. The red curves in Figure 1 depict the theoretical curves obtained by fitting the experimental J – V data (brown points)³⁷ to eq (1a) at room temperature ($T = 298.15$ K). As visible there, the agreement between the theoretical eq (1a) and experiment is excellent.

The fitting curves obtained via eq (1c) (assuming $T = 0$ K) are not shown; the difference from the exact (red) curves would be invisible within the drawing accuracy of Figure 1. Inspection of Table 1 reveals that the parameter values based on eq (1b) are very close to those based on eq (1a). This demonstrates that, definitely, thermal effects are altogether negligible for the presently envisaged EGaIn/F-nPT–Au large area junctions.

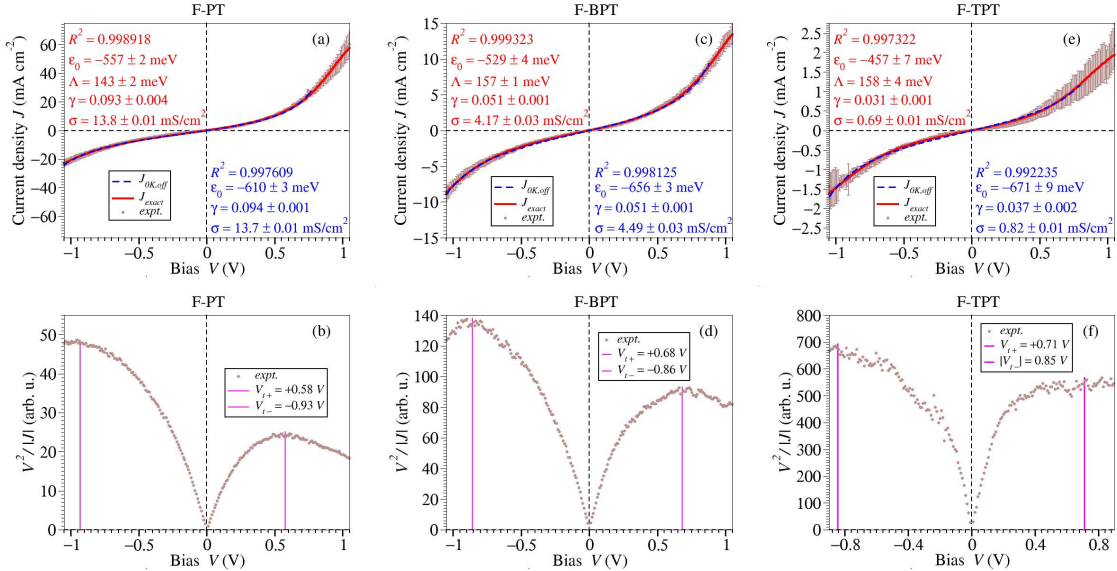


Figure 1: (a, c, e) Experimental J – V curves for fluorine terminated large area EGaIn/F-PT-Au, EGaIn/F-BPT-Au, and EGaIn/F-TPT-Au junctions containing one, two, or three phenyl rings, respectively (brown points, courtesy of Michael Zharnikov) from ref. 37 fitted to the exact eq (1a) (red lines). Fitting curves obtained via eq 1b) are not shown because they cannot be distinguished from the exact (red) curves within the drawing accuracy. Data fitting to eq (1c) (results depicted in blue) should employ a bias range compatible to this equation ($-1.2|V_{t-}| \lesssim V \lesssim 1.25V_{t+}$), where the transition voltages V_{t+} and $|V_{t-}|$ for positive and negative biases correspond to the maxima of the curve of $V^2/|J|$ versus V (panels b, d, and f).

The fitting curves obtained by using eq (1c) are drawn as blue lines in Figure 1. We will come

back to these curves at a later point in our analysis.

Table 1 shows that the magnitude of the HOMO energy offset $|\varepsilon_0|$ slightly decreases with increasing molecular size (number of phenyl rings n). This behavior is similar to that reported for CP-AFM junctions fabricated with (nonsubstituted) oligophenylys,²² but this does not represent the main concern of the present work. Rather, it is the dependence on the molecular size (number of phenyl rings n) of the other model parameters (namely $\bar{\Gamma}$ and Λ) that plays a central role in our analysis.

Table 1: Model parameter values obtained by fitting the experimental Au-F-nPT/EGaIn data³⁷ to the formula for the current indicated in the first column

Method	Property	F-PT	F-BPT	F-TPT
Eqs (1a)	ε_0	-557 ± 2	-529 ± 4	-457 ± 7
	Λ	143 ± 2	157 ± 1	158 ± 4
	γ	0.093 ± 0.004	0.051 ± 0.001	0.031 ± 0.001
	$\sigma (\beta = 1.5 \pm 0.2)$	13.8 ± 0.1	4.17 ± 0.03	0.69 ± 0.01
	R^2	0.998918	0.999323	0.997322
Eqs (1b)	ε_0	-550 ± 4	-519 ± 3	-455 ± 6
	Λ	149 ± 2	163 ± 1	158 ± 3
	γ	0.093 ± 0.001	0.051 ± 0.001	0.031 ± 0.001
	$\sigma (\beta = 1.5 \pm 0.2)$	14.1 ± 0.1	4.20 ± 0.03	0.71 ± 0.01
	R^2	0.998747	0.99929	0.9971
Eqs (1c)	ε_0	-610	-656	-671
	γ	0.094	0.051	0.037
	$\sigma (\beta = 1.4 \pm 0.2)$	13.7 ± 0.1	4.49 ± 0.03	0.82 ± 0.01
	R^2	0.997609	0.998125	0.992235
Ref. 37	Σ	3.9	4.1	4.6
	θ	48°	25.5°	21°
	ϕ	51°	68.5°	72.3°

The marked contrast between $\bar{\Gamma}$ and Λ shown in Figure 2 is an important finding reported in this work. As visible in Figure 2a, $\bar{\Gamma}$ exponentially decreases with n . Basically, it is this exponential decay of $\bar{\Gamma}$ that induces the exponential behavior of the low bias conductivity σ (Figure 2a). The same applies to the dependence on n of the current densities J at the biases $V = +0.5$ V and $V = -0.5$ V also presented in Figure 2a, similar to that already shown in ref. 37.

Were the HOMO width Λ merely the result of the HOMO-electrode couplings $\Gamma_{s,t}$ (i.e., $\Gamma_{env} \equiv 0$ in eq (4)), Λ would exhibit a similar exponential decay with n as $\bar{\Gamma}$, which is proportional to Γ_s and

Γ_t (cf. eq (3)). However, Figure 2b reveals that Λ is nearly independent of n (for not saying that it even slightly increases with n). This is a clear indication that Γ_s and Γ_t negligibly contribute to Λ , which appears to be dominated by the extrinsic term Γ_{env}

$$\Lambda \approx \Gamma_{env}/2 \quad (5)$$

Putting in more physical-chemical terms we arrive at another important finding presently reported. Eqs (5) implies that it is not the HOMO interaction with the electrodes that that determines the HOMO broadening but rather the interaction of a given molecule with its neighboring molecules of the SAM.

If so, Λ should be correlated with SAM properties. To demonstrate that this is indeed the case, we plotted in Figure 2c the values of Λ deduced by fitting the measured J - V curves (Table 1) against the average intermolecular distance $\langle d \rangle = \Sigma^{-1/2}$ expressed using the experimental values of the SAM coverage Σ (Figure 2c). We also show plots of Λ against the average tilt angle of the π^* orbitals ϕ and the average molecular tilt angle θ (both expressed with respect to the normal at surface) (Figure 2d).

The monotonic dependencies of Figures 2c and 2d convey an important message: more distant molecules in the SAM weaken the intra-SAM interactions which become less effective in broadening the HOMO density of states. This result provides microscopic support for the fact that, in the molecular junctions considered, the HOMO broadening is not dominated by the molecule-electrode interactions but rather by the intra-SAM interactions between neighboring molecules.

Before ending, a comment on the fitting curves obtained by using eq (1c) drawn as blue lines in Figure 1 is in order. As seen in Figures 1a, c, and e, these (blue) curves also reproduce well the experimental measurements in the bias range $(-1.2|V_{t-}| \lesssim V \lesssim 1.2V_{t+})$ where eq (1c) applies.^{43,44} Here, V_{t+} and V_{t-} are transition voltage for positive and negative bias polarities, which are defined by the maxima of the curves for $V^2/|J|$ (Figures 1b, d, and f). As visible in Table 1 and Figures 1a,

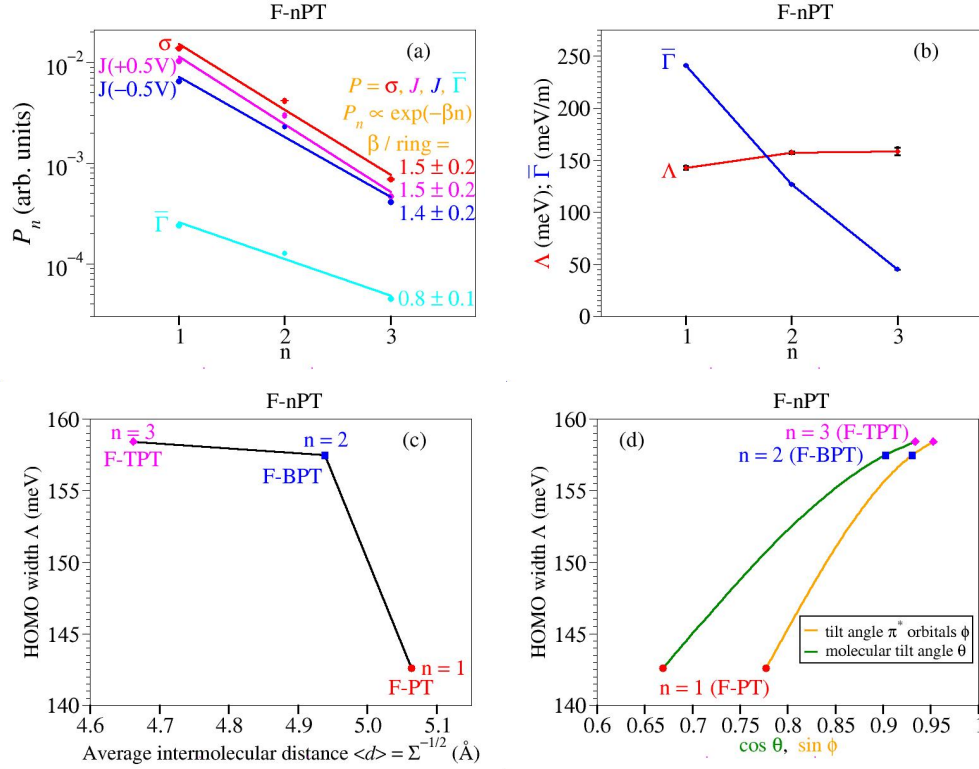


Figure 2: (a) Exponential fall-off with the number of the phenyl rings n of the properties (P_n) indicated in the legend: conductivity (σ), current densities J at ± 0.5 V, and the quantity $\bar{\Gamma}$ proportional to the effective MO coupling to electrodes Γ . (b) The weak dependence of the model parameters ϵ_0 and Λ on the repeat phenyl units n contrasting with the strong dependence of $\bar{\Gamma}$ on n . Dependence of the HOMO width Λ (c) on the average intermolecular distance d expressed in terms of the SAM coverage Σ and (d) on the π^* orbital tilt angle ϕ and molecular tilt angle θ . The lines in panel a represent linear data fitting, those of panels b, c and d are guide to the eye.

c, and e, the MO offset $|\epsilon_0|$ obtained using eq (1c) are somewhat overestimated compared to those obtained using the exact eq (1a). The reason is that, to be accurate, the off-resonance condition underlying eq (1c) does not only imply biases sufficiently away from resonance ($e|V| = 2|\epsilon_V|$) but also $\Lambda \lesssim |\epsilon_0|/10$.⁴⁴ The latter condition is not satisfied by the values of Table 1, and for this reason, the estimates for ϵ_0 based eq (1c) are not so accurate as in many other cases investigated earlier.^{3,4,6–29}

In closing, in this Letter we demonstrated that, notwithstanding the potential action as charge trap of the terminal F atom they contain,^{39–42} large area molecular junctions fabricated with fluorine terminated oligophenyls and EGaIn top electrodes (i) exhibit transport properties that can be

excellently reproduced using a recently deduced analytic formula for the current based on a single level (MO) model, which reveals (ii) that HOMO-electrode coupling Γ and the HOMO broadening Λ have different physical-chemical origins, and (iii) that, rather than being dominated by molecule-electrode interaction, the HOMO broadening is basically due to intra-SAM interactions, as witnessed by the correlation of Λ with the properties of the SAM (coverage and tilt angles).

From a methodological perspective, the present work is a plea in favor of investigating junctions fabricated using homologous molecular series rather than disparate molecular species. In arriving at conclusions (ii) and (iii) mentioned above, pursuing this route was essential.

This research did not receive any specific financial support but benefited from computational support by the state of Baden-Württemberg through bwHPC and the German Research Foundation through Grant No. INST 40/575-1 FUGG (bwUniCluster 2, bwForCluster/HELIX, and JUSTUS 2 cluster).

Conflicts of interest

There are no conflicts to declare.

References

- (1) Hall, L. E.; Reimers, J. R.; Hush, N. S.; Silverbrook, K. Formalism, Analytical Model, and a Priori Green's-Function-Based Calculations of the Current-Voltage Characteristics of Molecular Wires. *J. Chem. Phys.* **2000**, *112*, 1510–1521.
- (2) Peterson, I. R.; Vuillaume, D.; Metzger, R. M. Analytical Model for Molecular-Scale Charge Transport. *J. Phys. Chem. A* **2001**, *105*, 4702–4707.
- (3) Smaali, K.; Clément, N.; Patriarche, G.; Vuillaume, D. Conductance Statistics from a Large Array of Sub-10 nm Molecular Junctions. *ACS Nano* **2012**, *6*, 4639–4647.

- (4) Tran, T. K.; Smaali, K.; Hardouin, M.; Bricaud, Q.; Oçafraïn, M.; Blanchard, P.; Lenfant, S.; Godey, S.; Roncali, J.; Vuillaume, D. A Crown-Ether Loop-Derivatized Oligothiophene Doubly Attached on Gold Surface as Cation-Binding Switchable Molecular Junction. *Adv. Mater.* **2013**, *25*, 427–431.
- (5) Bâldea, I. Interpretation of Stochastic Events in Single-Molecule Measurements of Conductance and Transition Voltage Spectroscopy. *J. Am. Chem. Soc.* **2012**, *134*, 7958–7962.
- (6) Fracasso, D.; Muglali, M. I.; Rohwerder, M.; Terfort, A.; Chiechi, R. C. Influence of an Atom in EGaIn/Ga₂O₃ Tunneling Junctions Comprising Self-Assembled Monolayers. *J. Phys. Chem. C* **2013**, *117*, 11367–11376.
- (7) Guo, S.; Zhou, G.; Tao, N. Single Molecule Conductance, Thermopower, and Transition Voltage. *Nano Lett.* **2013**, *13*, 4326–4332.
- (8) Wu, K.; Bai, M.; Sanvito, S.; Hou, S. Quantitative Interpretation of the Transition Voltages in Gold-Poly(phenylene) Thiol-Gold Molecular Junctions. *J. Chem. Phys.* **2013**, *139*, 194703.
- (9) Lo, W.-Y.; Bi, W.; Li, L.; Jung, I. H.; Yu, L. Edge-on Gating Effect in Molecular Wires. *Nano Lett.* **2015**, *15*, 958–962.
- (10) Xiang, A.; Wang, M.; Wang, H.; Sun, H.; Hou, S.; Liao, J. The Origin of the Transition Voltage of Gold-Alkanedithiol-Gold Molecular Junctions. *Chem. Phys.* **2016**, *465-466*, 40–45.
- (11) Nose, D.; Dote, K.; Sato, T.; Yamamoto, M.; Ishii, H.; Noguchi, Y. Effects of Interface Electronic Structures on Transition Voltage Spectroscopy of Alkanethiol Molecular Junctions. *J. Phys. Chem. C* **2015**, *119*, 12765–12771.
- (12) Kovalchuk, A.; Abu-Husein, T.; Fracasso, D.; Egger, D.; Zojer, E.; Zharnikov, M.; Terfort, A.; Chiechi, R. Transition Voltages Respond to Synthetic Reorientation of Embedded Dipoles in Self-Assembled Monolayers. *Chem. Sci.* **2015**, *7*, 781–787.

- (13) Jia, C. et al. Covalently Bonded Single-Molecule Junctions with Stable and Reversible Photoswitched Conductivity. *Science* **2016**, *352*, 1443–1445.
- (14) Xiang, D.; Wang, X.; Jia, C.; Lee, T.; Guo, X. Molecular-Scale Electronics: From Concept to Function. *Chem. Rev.* **2016**, *116*, 4318–4440.
- (15) Wang, Q.; Liu, R.; Xiang, D.; Sun, M.; Zhao, Z.; Sun, L.; Mei, T.; Wu, P.; Liu, H.; Guo, X.; Li, Z.-L.; Lee, T. Single-Atom Switches and Single-Atom Gaps Using Stretched Metal Nanowires. *ACS Nano* **2016**, *10*, 9695–9702.
- (16) Jeong, H.; Jang, Y.; Kim, D.; Hwang, W.-T.; Kim, J.-W.; Lee, T. An In-Depth Study of Redox-Induced Conformational Changes in Charge Transport Characteristics of a Ferrocene-Alkanethiolate Molecular Electronic Junction: Temperature-Dependent Transition Voltage Spectroscopy Analysis. *J. Phys. Chem. C* **2016**, *120*, 3564–3572.
- (17) Li, L.; Lo, W.-Y.; Cai, Z.; Zhang, N.; Yu, L. Proton-Triggered Switch Based on a Molecular Transistor with Edge-on Gate. *Chem. Sci.* **2016**, *7*, 3137–3141.
- (18) Lo, W.-Y.; Zhang, N.; Cai, Z.; Li, L.; Yu, L. Beyond Molecular Wires: Design Molecular Electronic Functions Based on Dipolar Effect. *Acc. Chem. Res.* **2016**, *49*, 1852–1863.
- (19) Yi, X.; Izarova, N. V.; Stuckart, M.; Guérin, D.; Thomas, L.; Lenfant, S.; Vuillaume, D.; van Leusen, J.; Duchoň, T.; Nemšák, S.; Bourone, S. D. M.; Schmitz, S.; Kögerler, P. Probing Frontier Orbital Energies of Co₉(P₂W₁₅)₃ Polyoxometalate Clusters at Molecule–Metal and Molecule–Water Interfaces. *J. Am. Chem. Soc.* **2017**, *139*, 14501–14510.
- (20) Cai, Z.; Zhang, N.; Awais, M. A.; Filatov, A. S.; Yu, L. Synthesis of Alternating Donor-Acceptor Ladder-Type Molecules and Investigation of Their Multiple Charge-Transfer Pathways. *Angew. Chem. Int. Ed.* **2018**, *57*, 6442–6448.
- (21) Jeong, I.; Song, H. Transition Voltage Spectroscopy Analysis of Charge Transport through Molecular Nanojunctions. *Appl. Spectr. Rev.* **2018**, *53*, 246–263.

- (22) Xie, Z.; Bâldea, I.; Frisbie, C. D. Determination of Energy Level Alignment in Molecular Tunnel Junctions by Transport and Spectroscopy: Self-Consistency for the Case of Oligophenylene Thiols and Dithiols on Ag, Au, and Pt Electrodes. *J. Am. Chem. Soc.* **2019**, *141*, 3670–3681.
- (23) Xie, Z.; Bâldea, I.; Frisbie, C. D. Energy Level Alignment in Molecular Tunnel Junctions by Transport and Spectroscopy: Self-Consistency for the Case of Alkyl Thiols and Dithiols on Ag, Au, and Pt Electrodes. *J. Am. Chem. Soc.* **2019**, *141*, 18182–18192.
- (24) Nguyen, Q. V.; Xie, Z.; Frisbie, C. D. Quantifying Molecular Structure-Tunneling Conductance Relationships: Oligophenylene Dimethanethiol vs Oligophenylene Dithiol Molecular Junctions. *J. Phys. Chem. C* **2021**, *125*, 4292–4298.
- (25) Gu, M.-W.; Peng, H. H.; Chen, I.-W. P.; Chen, C.-H. Tuning Surface d Bands with Bimetallic Electrodes to Facilitate Electron Transport across Molecular Junctions. *Nat. Mater.* **2021**, *20*, 658–664.
- (26) Liu, Y.; Qiu, X.; Soni, S.; Chiechi, R. C. Charge Transport through Molecular Ensembles: Recent Progress in Molecular Electronics. *Chem. Phys. Rev.* **2021**, *2*, 021303.
- (27) Kim, Y.; Im, K.; Song, H. Charge Transport Characteristics of Molecular Electronic Junctions Studied by Transition Voltage Spectroscopy. *Materials* **2022**, *15*, 774.
- (28) Carlotti, M.; Soni, S.; Kovalchuk, A.; Kumar, S.; Hofmann, S.; Chiechi, R. C. Empirical Parameter to Compare Molecule-Electrode Interfaces in Large-Area Molecular Junctions. *ACS Phys. Chem. Au* **2022**, *2*, 179–190.
- (29) Jang, J.; He, P.; Yoon, H. J. Molecular Thermoelectricity in EGaIn-Based Molecular Junctions. *Acc. Chem. Res.* **2023**, *56*, 1613–1622.
- (30) Zotti, L. A.; Kirchner, T.; Cuevas, J.-C.; Pauly, F.; Huhn, T.; Scheer, E.; Erbe, A. Reveal-

- ing the Role of Anchoring Groups in the Electrical Conduction Through Single-Molecule Junctions. *Small* **2010**, *6*, 1529–1535.
- (31) Xie, Z.; Bâldea, I.; Smith, C.; Wu, Y.; Frisbie, C. D. Experimental and Theoretical Analysis of Nanotransport in Oligophenylene Dithiol Junctions as a Function of Molecular Length and Contact Work Function. *ACS Nano* **2015**, *9*, 8022–8036.
- (32) Bâldea, I. Estimating the Number of Molecules in Molecular Junctions Merely Based on the Low Bias Tunneling Conductance at Variable Temperature. *Int. J. Mol. Sci.* **2022**, *23*, 14985.
- (33) Bâldea, I. Can Tunneling Yield a Current in Molecular Junctions so Strongly Temperature Dependent to Challenge a Hopping Mechanism? General Analytical Formulas that Answer This Question Positively. *Phys. Chem. Chem. Phys.* **2024**, DOI 10.1039/D3CP05046G.
- (34) Abramowitz, M., Stegun, I. A., Eds. *Handbook of Mathematical Functions with Formulas, Graphs, and Mathematical Tables.*; National Bureau of Standards Applied Mathematics Series, U.S. Government Printing Office, Washington, D.C., 1964.
- (35) Yoon, H. J.; Bowers, C. M.; Baghbanzadeh, M.; Whitesides, G. M. The Rate of Charge Tunneling Is Insensitive to Polar Terminal Groups in Self-Assembled Monolayers in AgTSS(CH₂)_nM(CH₂)_mT//Ga₂O₃/EGaIn Junctions. *J. Am. Chem. Soc.* **2014**, *136*, 16–19.
- (36) Sangeeth, C. S. S.; Demissie, A. T.; Yuan, L.; Wang, T.; Frisbie, C. D.; Nijhuis, C. A. Comparison of DC and AC Transport in 1.5-7.5 nm Oligophenylene Imine Molecular Wires across Two Junction Platforms: Eutectic Ga-In versus Conducting Probe Atomic Force Microscope Junctions. *J. Am. Chem. Soc.* **2016**, *138*, 7305–7314.
- (37) Liu, Y.; Katzbach, S.; Asyuda, A.; Das, S.; Terfort, A.; Zharnikov, M. Effect of Substitution on the Charge Transport Properties of Oligophenylenethiolate Self-Assembled Monolayers. *Phys. Chem. Chem. Phys.* **2022**, *24*, 27693–27704.

- (38) Kong, G. D.; Kim, M.; Jang, H.-J.; Liao, K.-C.; Yoon, H. J. Influence of Halogen Substitutions on Rates of Charge Tunneling across SAM-based Large-Area Junctions. *Phys. Chem. Chem. Phys.* **2015**, *17*, 13804–13807.
- (39) Doyon, B.; Andrei, N. Universal Aspects of Nonequilibrium Currents in a Quantum Dot. *Phys. Rev. B* **2006**, *73*, 245326.
- (40) Mehta, P.; Andrei, N. Nonequilibrium Transport in Quantum Impurity Models: The Bethe Ansatz for Open Systems. *Phys. Rev. Lett.* **2006**, *96*, 216802, See also erratum, cond-mat/0703426.
- (41) Doyon, B. New Method for Studying Steady States in Quantum Impurity Problems: The Interacting Resonant Level Model. *Phys. Rev. Lett.* **2007**, *99*, 076806.
- (42) Bâldea, I. Effects of Stochastic Fluctuations at Molecule-Electrode Contacts in Transition Voltage Spectroscopy. *Chem. Phys.* **2012**, *400*, 65–71.
- (43) Bâldea, I. Ambipolar Transition Voltage Spectroscopy: Analytical Results and Experimental Agreement. *Phys. Rev. B* **2012**, *85*, 035442.
- (44) Bâldea, I. Can Room Temperature Data for Tunneling Molecular Junctions Be Analyzed within a Theoretical Framework Assuming Zero Temperature? *Phys. Chem. Chem. Phys.* **2023**, *25*, 19750–19763.